

# Prototype Tests and Construction of the Hadron Blind Detector for the PHENIX Experiment

C.Woody, W.Anderson, B.Azmoun, C.-Y. Chi, A.Drees, A.Dubey, M.Durham, Z.Fraenkel, J.Harder, T.Hemmick, R.Hutter, B.Jacak, J.Kamin, A.Kozlov, A.Milov, M.Naglis, P.O'Connor, R.P.Pisani, V.Radeka, I.Ravinovich, T.Sakaguchi, D.Sharma, L.Shekhtman, A.Sickles, S.Stoll, I.Tserruya, B.Yu

**Abstract**— A Hadron Blind Detector (HBD) has been constructed as part of the detector upgrade program for the PHENIX experiment at RHIC. The HBD is a proximity focused windowless Cherenkov detector operated with pure  $\text{CF}_4$  that will be used to detect single and double electrons in relativistic heavy ion collisions and provide additional rejection power against Dalitz pairs and photon conversions. The detector consists of a 50 cm long radiator directly coupled to a set of triple GEM detectors equipped with CsI photocathodes to detect UV photons produced by electrons emitting Cherenkov light. A full scale prototype of the HBD was built and tested in order to study its performance under beam conditions. Tests with the prototype demonstrated good separation between electrons and hadrons using pulse height discrimination and cluster size. The final detector has now been constructed and installed in PHENIX and is presently undergoing commissioning in preparation for its first round of data taking during the next heavy ion run at RHIC. Results of the beam test of the prototype, as well as on the construction and initial testing of the final detector, are presented in this paper.

## I. INTRODUCTION

A Hadron Blind Detector (HBD) has been constructed as part of the upgrade program for the PHENIX Experiment at the Relativistic Heavy Ion Collider (RHIC) at BNL [1]. The HBD will allow the measurement of electron-positron pairs from the decay of the light vector mesons ( $\rho$ ,  $\omega$  and  $\phi$ ) and the low-mass pair continuum in Au-Au collisions at energies up to  $\sqrt{s_{NN}} = 200$  GeV.

The device is a windowless Cherenkov detector using pure  $\text{CF}_4$  as a radiator in a proximity focus configuration utilizing a set of triple GEM detectors equipped with cesium iodide (CsI) photocathodes. The photocathode is evaporated on the top

surface of the uppermost GEM which produces photoelectrons that are amplified with a gain of  $\sim 5 \times 10^3$  by the GEM detector. The combination of a windowless detector with the CsI photocathode and  $\text{CF}_4$  results in a very large bandwidth (from 6 to 11.5 eV) and a very high figure of merit ( $N_0 \sim 840 \text{ cm}^{-1}$ ). One expects approximately 36 detected photoelectrons with a 50 cm long radiator, which ensures a high level of single electron efficiency and double hit recognition. Electrons traversing the radiator produce Cherenkov light in the form of a “blob” on a pad readout plane with a pad size approximately equal to the blob size ( $\sim 10 \text{ cm}^2$ ) resulting in a low granularity detector.

A significant R&D program was carried out to develop the various components of this detector that has now been completed [2,3]. A prototype detector was constructed to test the key parameters of the device and to measure its performance under actual test beam conditions. The final detector has now been constructed and installed in PHENIX, and is undergoing commissioning in preparation for its first round of data taking during the upcoming run at RHIC.

## II. THE HBD CONCEPT

Figure 1 shows the configuration of the triple GEM detectors used in the HBD. The CsI photocathode is deposited on the upper surface of the top GEM and a bias voltage is applied between the top GEM and the mesh. Depending on the direction of the bias field, charge produced by ionizing particles in the upper gap can either be collected by the GEM (FB = Forward Bias), or by the mesh (RB = Reverse Bias). In either configuration, photoelectrons produced on the photocathode are collected with good efficiency into the GEM due the strong electric field near the holes. Only a very small amount of ionization charge produced very near the photocathode (within  $\sim 100 \mu\text{m}$ ) is collected by the GEM. The Forward Bias mode is therefore sensitive to hadrons and other charged particles, while the Reverse Bias mode is essentially sensitive only to Cherenkov light produced by electrons (hence the term “Hadron Blind”). Numerous tests were carried out in the lab to study the effect of suppressing the charge collected in negative bias mode and how the reverse bias voltage effects the photoelectron collection efficiency. These tests are described in detail in Refs [2] and [3].

---

Manuscript submitted on November 19, 2006. This work was supported in part by the U.S. Department of Energy under Prime Contract No. DE-AC02-98CH10886.

A.Dubey, Z.Fraenkel, A.Kozlov, M.Naglis, D.Sharma, I.Ravinovich, L.Shekhtman and I.Tserruya, are with the Department of Particle Physics, Weizmann Institute of Science, Rehovot, Israel

B.Azmoun, A.Milov, R.P.Pisani, T.Sakaguchi, A.Sickles, S.Stoll and C.Woody\* are with the Physics Department at Brookhaven National Laboratory, Upton, NY (\*Contact author: E-mail: woody@bnl.gov).

J.Harder, P.O'Connor, V.Radeka and B.Yu are with the Instrumentation Division at Brookhaven National Laboratory, Upton, NY

W.Anderson, A.Drees, M.Durham, T.Hemmick, R.Hutter, B.Jacak, and J.Kamin are with the Physics Department, Stony Brook University, Stony Brook, NY.

C.-Y. Chi is with Nevis Labs, Columbia University, Irvington, NY.

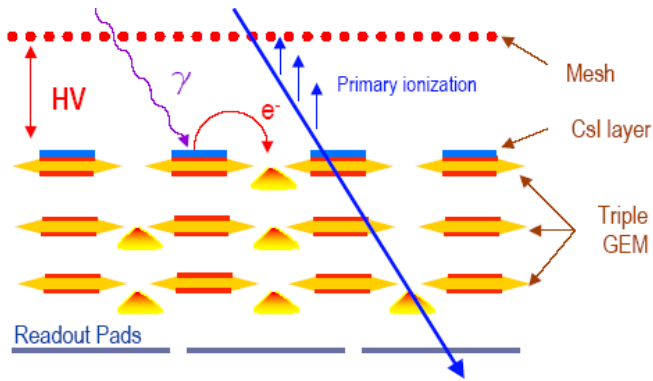


Fig. 1 Configuration of GEM detectors and CsI photocathodes in the HBD. With a higher negative voltage on the mesh than on the top GEM (Forward Bias), electrons produced in the top gap are collected by the GEM. With a lower negative voltage on the mesh than on the top GEM, ionization electrons are collected by the mesh (Negative Bias), and the detector is “Hadron Blind”.

### III. DETECTOR CONSTRUCTION

#### A. Vessel

The HBD vessel was designed and built at the Weizmann Institute of Science in Rehovot, Israel. It consists of a thin honeycomb structure for the outer vessel, which constitutes about 3% of a radiation length of material inside the fiducial acceptance of PHENIX, including the gas radiator. The detector is divided into two halves, one of which is shown in Fig. 2. Each half contains twelve triple GEM modules, each consisting of one gold plated GEM on the top and two standard GEMs below. The dimension of each GEM is approximately 23 x 27 cm<sup>2</sup>. All GEMs were produced at CERN. Out of a total of 133 foils produced, 65 standard GEMs and 47 gold plated GEMs passed all quality assurance tests. Forty eight standard GEMs and 24 gold plated GEMs were used to construct the final detector.

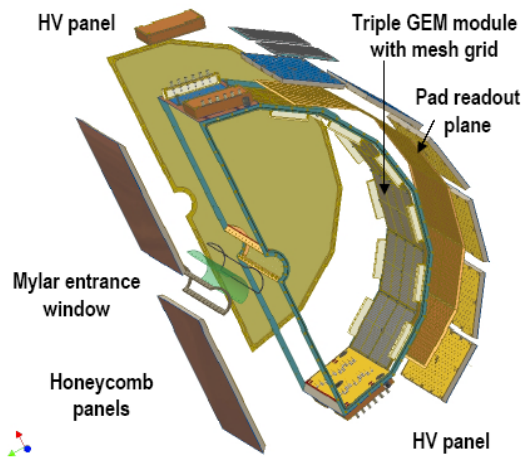


Fig. 2 Exploded view of one of the HBD vessels.

#### B. GEM modules

Each GEM was tested individually and then matched in groups of three in order to give the lowest possible gain variation for all modules in the detector. The resulting gain spread from module to module varied from 5-20%. Each module was then mapped in order to study the gain variation within a module. The gain was measured with an <sup>55</sup>Fe source which produced a rate of ~ 8 KHz. The source was initially placed over one pad and the gain was measured as a function of time in the same location for approximately half an hour. During this time, the gain was observed to increase by anywhere between a few percent to up to a factor of two depending on the module before, reaching a steady plateau. This effect is shown in Fig. 3 for a module which exhibited a gain increase of about a factor of 1.5. This behavior is typical of many GEM detectors and is believed to be due to an initial charging up effect due to polarization of the polyimide foils when the high voltage is initially applied.

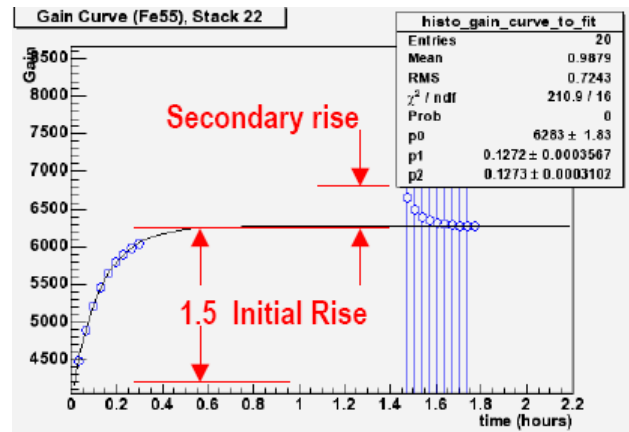


Fig. 3 Gain variation of a triple GEM module during gain mapping. The initial rise is typical of most GEM detectors and varied between a few percent and a factor of two depending on the module.

The source was then moved to measure all the other pads with the module and then returned to its original position where the gain was measured again. The gain was typically higher at the beginning of this second measurement, but then decreased to the original plateau established during the initial charge up period. We also found that the rates of gain increase and decrease were somewhat different (the discharge rate was approximately a factor of two shorter than the charging up rate), and the charging up rate was slightly rate dependent (~ 10-30% for rates between 10Hz – 8 KHz). However, once the operating plateau was reached, the gain appeared to be stable.

### C. Photocathode production

The photocathodes for the HBD were produced at Stony Brook University in a “Clean Tent” that allowed both fabrication of the photocathodes using a high vacuum evaporator system, as well as assembly of the detector under very clean and dry conditions (typically Class 10-100). Figure 4 shows the Clean Tent at Stony Brook, which contained the evaporator seen in the back, a large, high quality glove box, a laminar flow hood, a high vacuum storage container for the GEMs, and numerous other auxiliary pieces of equipment.



Fig. 4 The “Clean Tent” at Stony Brook University where the CsI photocathodes were produced and the final detector was assembled. The high vacuum evaporator is located at the back of the tent, with the glove box on the right and the laminar flow table on the left in the back.

The evaporator was originally constructed by the INFN and the Instituto Superiore di Sanita in Rome, Italy and is presently on loan to Stony Brook University [4]. This is a very sophisticated and high quality apparatus that is capable of producing four HBD photocathodes at a time, along with several small “chicklets” that were used for monitoring the photocathode quality. GEM foils are mounted into an open aluminum box and placed inside the evaporator which deposits a thin layer of CsI on the top surface of the GEM. The rate of deposition was  $\sim 20$  A/sec and the total thickness of the final layer was between 2400-4500 Å. The vacuum inside the evaporator was typically  $10^{-7}$  torr during evaporation. The quantum efficiency of the photocathode was then measured in situ inside the evaporator over the entire area of the GEM using a remote controlled movable UV light source and current monitor. The quantum efficiency was measured over the entire area of the photocathode at several wavelengths from 165-200 nm, while the test “chicklets” were measured over the wavelength range from 120-200 nm in a separate monochromator. Fig. 5 shows a position scan for a typical photocathode, which shows good uniformity across nearly the entire foil. Fig. 6 shows the quantum efficiency measured for one of the chicklets compared to a good quality photocathode produced at the Weizmann Institute. In general, all of the photocathodes produced were of excellent quality and showed very good uniformity.

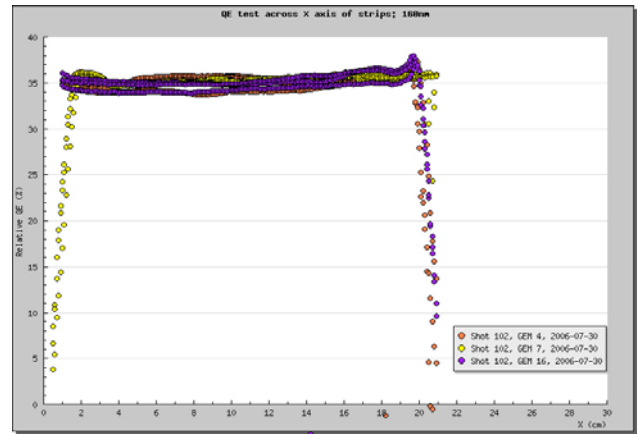


Fig. 5 Spatial uniformity of several typical photocathodes produced in the Stony Brook evaporator.

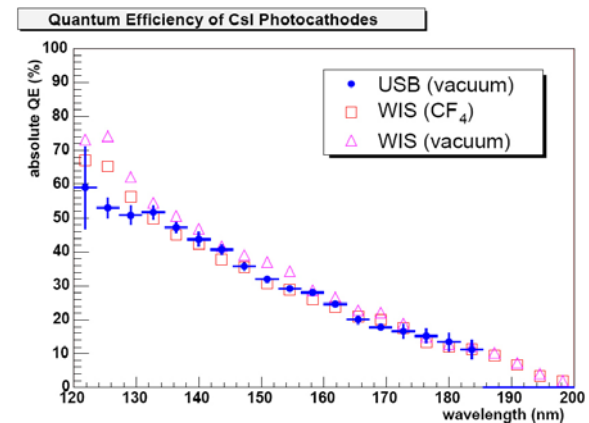


Fig. 6 Quantum efficiency as a function of wavelength of a photocathode produced in the evaporator at Stony Brook compared to a known good photocathode produced at the Weizmann Institute. Measurements made at Stony Brook were done in vacuum. Measurements at the Weizmann were done in vacuum and  $CF_4$ .

The photocathodes were sealed inside a gas tight aluminum box while still inside the evaporator and then transferred to the glove box. The photocathodes were therefore never exposed to air at any time during this process. The glove box atmosphere of nitrogen was kept extremely dry and oxygen free ( $O_2 < 5$  ppm and  $H_2O < 10$  ppm). The photocathodes were installed into the detector and electrically tested along with all of the other GEMs. Fig. 7 shows the first half of the HBD with all of its photocathodes installed while still in the glove box. After all of the photocathodes and GEM modules were installed, the detector was sealed and removed from the glove box where it was put under its own gas flow of argon or nitrogen.

Once outside the glove box, circuit boards containing the readout electronics were installed on the back side of the vessel. These boards contained the preamplifiers that are connected to the readout pads inside the detector via a series of short, individual wires that pass through the honeycomb wall of the vessel and are soldered to the input pads of the preamps.

The preamps were designed by the Instrumentation Division at Brookhaven (IO-1195) and produce a differential signal in the range from 0 to  $\pm 1V$  that is delivered to a receiver and front end module designed by Nevis labs. The front end module contains a 12 bit, 65 MHz ADC for each channel which digitizes the signal and sends the data via an optical G-Link to the PHENIX data acquisition system.

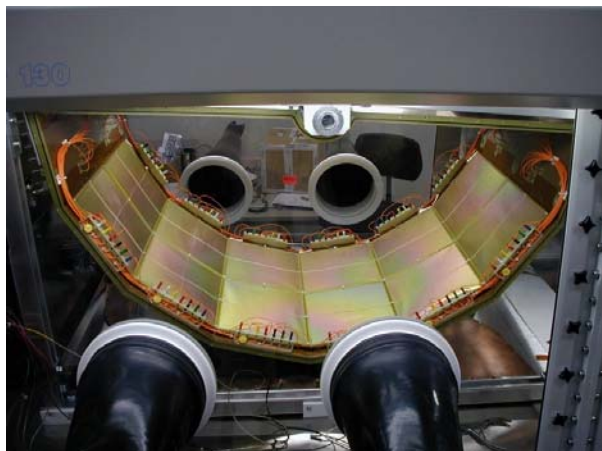


Fig. 7 One half of the final HBD detector with all CsI photocathodes and GEM modules installed inside the glove box used for assembly.

#### IV. FINAL DETECTOR INSTALLATION

The final detector was installed into the PHENIX experiment during the fall of this year. Figure 8 shows the west detector which was installed in early September. The two square panels on the front face of the detector are heater foils that are described in the next section. The east detector was installed approximately one month later, surrounding the beam pipe.

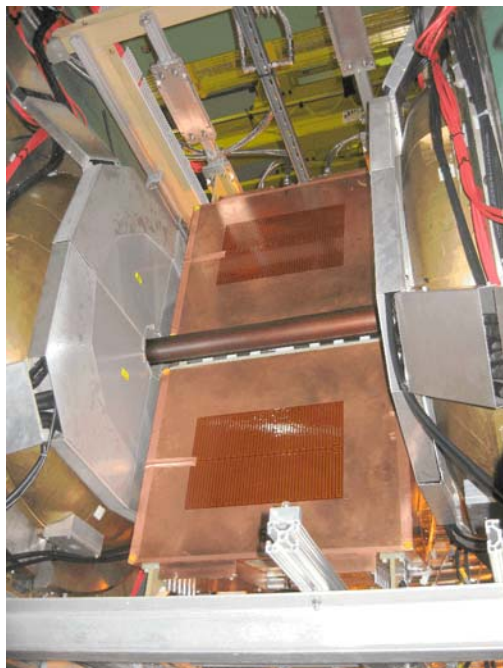


Fig. 8 HBD west detector installed in PHENIX

#### V. HIGH PURITY GAS SYSTEM

It is extremely important to maintain low water and oxygen levels in the operating gas of the final detector. Both water and oxygen have absorption bands in the deep UV that would absorb Cherenkov light and reduce the overall photoelectron yield [5]. Every 10 ppm of either oxygen or water results in a loss of approximately 1 photoelectron due to absorption in the 50 cm gas radiator. In addition, water will adversely affect the photocathode performance and reduce its quantum efficiency.

In order to maintain the highest purity operating gas in the final detector, the HBD gas system in PHENIX has been constructed using all stainless steel tubing and valves, and with components which are free of silicon, grease or any materials that are prone to out gassing. Both water and oxygen are monitored continuously for the common input gas, and independently for the output gas from each half of the detector.

While the input gas can be kept very pure, out gassing of water can occur from inside the detector due to the release of trapped water from the GEM foils, the kapton readout plane and the FR4 frames of the vessel. External heater foils were installed on the outside surfaces of the vessel which can be used to raise the temperature inside to  $\sim 40$  deg C in order to drive out as much water as possible in a conditioning mode before the detector is actually operated for physics data taking. This process has been very successful, and the present water levels are down to  $\sim 10-15$  ppm in the final installation and are expected to further improve before data taking begins.

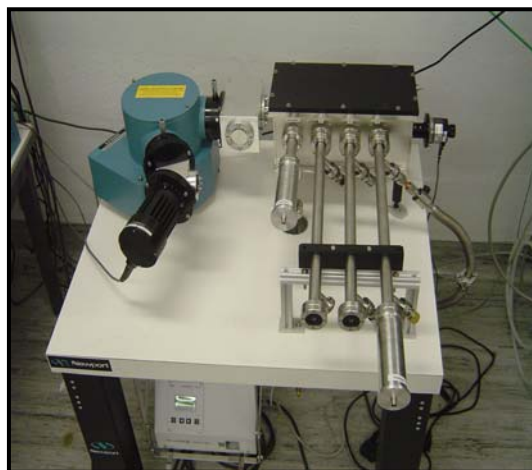


Fig. 9 Gas transmission monitor system partially constructed. From left to right: D<sub>2</sub> lamp and scanning monochromator, beam splitter box, reference PMT, gas test cells (one input, two output) with one PMT mounted..

In addition to monitoring the water and oxygen levels, we have constructed a gas transmission monitor that will measure the UV transmission of the input and output gas from both halves of the detector. This will not only serve to verify the absorbance caused by oxygen and water, but will also identify any other possible contaminants in the gas which could cause absorption of the Cherenkov light. The system consists of a scanning VUV monochromator (McPherson 234/302 with D<sub>2</sub>

lamp) with a beam splitter box containing a movable mirror that directs a beam of light down three independent gas test cells (one input, two output). The light impinges on photomultiplier tubes (Hamamatsu R6835) with CsI photocathodes operated in photodiode mode and the photocurrent is measured using a Keithley picoammeter. Fig 9 shows the partially assembled spectrometer which will be completed and installed in PHENIX within the next few weeks.

## VI. PROTOTYPE TESTS

A full scale prototype of the HBD was built and tested under beam conditions (200 GeV pp collisions) in the PHENIX experiment at RHIC during the spring and early summer of this year. The detector showed stable operation with pure CF<sub>4</sub> as the operating gas and worked well in the RHIC environment. The detector also demonstrated the expected performance in terms of “hadron blindness”. Figure 10 shows the pulse height distribution for minimum ionizing particles obtained with the detector in forward bias (FB) mode and reverse bias (RB) modes. The forward bias distribution shows a clear minimum ionizing peak and is well fit with a Landau distribution. The reverse bias mode shows the strong suppression of the direct ionization signal, as expected.

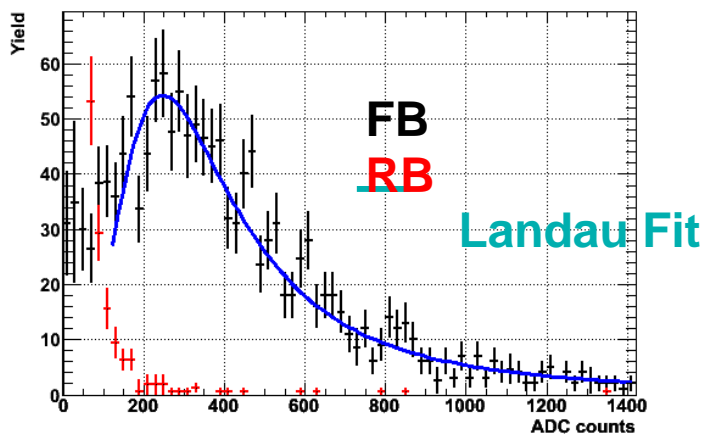


Fig. 10 Pulse height distribution for minimum ionizing particles obtained with the full scale HBD prototype operating in the PHENIX experiment at RHIC. The forward bias distribution is well fit with a Landau distribution, while the reverse bias distribution shows the expected strong suppression of the direct ionization signal.

Figure 11 shows the pulse height distribution and cluster size for electrons and hadrons obtained with the prototype detector under reverse bias conditions. The electrons and hadrons were both well identified using other detectors in PHENIX. The electron distribution is well separated from the hadron signal and gives approximately a 15:1 rejection factor with an electron efficiency of 90% using a simple pulse height cut alone. The cluster size distribution shows a much larger average cluster size for electrons, and will be used to further increase the rejection power in the final analysis

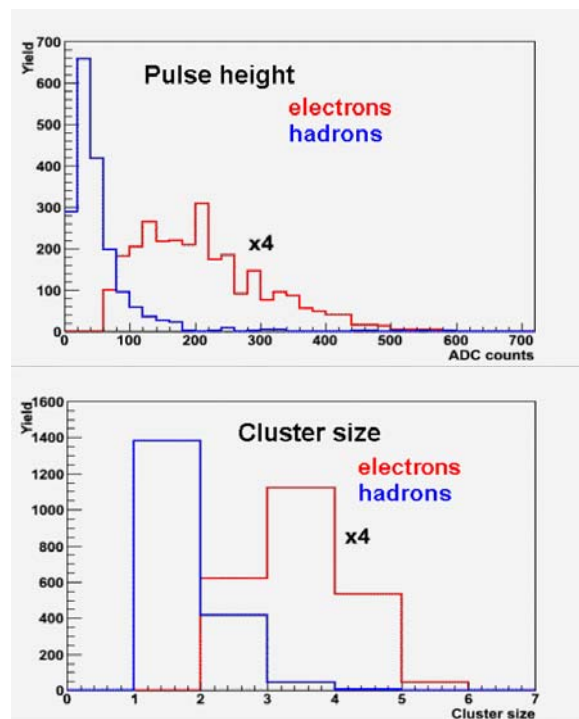


Fig. 11. Pulse height distribution (a) and cluster size distribution (b) for identified electrons and hadrons with the HBD prototype operated in reverse bias mode in PHENIX during the last RHIC run.

## VII. SUMMARY

A novel new Hadron Blind Detector has been constructed for the PHENIX experiment that will greatly enhance the capability to measure low mass electron pairs at RHIC. A test with a full scale prototype detector was carried out during the spring of this year and demonstrated the hadron blindness feature of the HBD concept under actual running conditions. The construction and assembly of the final detector was completed during this past summer, and both halves of the final detector have now been installed in PHENIX and are undergoing preparations and commissioning for the upcoming run at RHIC.

## VIII. REFERENCES

- [1] B.Azmoun et.al., “Conceptual Design Report on a HBD Upgrade for the PHENIX Detector”, March 2005, [http://www.phenix.bnl.gov/WWW/TPCHBD/HBD\\_CDR.pdf](http://www.phenix.bnl.gov/WWW/TPCHBD/HBD_CDR.pdf)
- [2] A.Kozolov et.al., “Development of a Triple GEM UV Photon Detector Operated in Pure CF<sub>4</sub> for the PHENIX Experiment”, Nucl. Inst. Meth. A523 (2004) 345.
- [3] Z.Frankel et.al., “A Hadron Blind Detector for the PHENIX Experiment at RHIC”, Nucl. Inst. Meth. A546 (2005) 466-480.
- [4] Evaporation facility provided by the INFN and Instituto Superiore di Sanatia in Rome, Italy, courtesy of Prof. F. Giribaldi and collaborators at Jefferson Lab
- [5] I.Tserruya et.al., “A Hadron Blind Detector for the PHENIX Experiment at RHIC”, Conference Record Proceedings of the 2004 IEEE Nuclear Science Symposium and Medical Imaging Conference, Oct 16-22, 4004, Rome, Italy.